Int J Adv Manuf Technol (2012) 62:1013–1023
DOI 10.1007/s00170-011-3745-0

ORIGINAL ARTICLE

Evaluation of the characteristics of the microelectrical discharge machining process using response surface methodology based on the central composite design

Y. C. Lin · C. C. Tsao · C. Y. Hsu · S. K. Hung · D. C. Wen

Received: 17 August 2011 / Accepted: 3 November 2011 / Published online: 17 November 2011

Abstract Evaluation of the characteristics of a micro-electrical discharge machining (Micro-EDM) process is challenging, because it involves complex, interrelated relationships so a proper modeling approach is necessary to clearly identify the crucial machining variables and their interrelationships in order to initiate more effective strategies to improve Micro-EDM qualities (electrode wear (EW), material removal rate (MRR) and overcut). This paper uses a response surface method (RSM) based on the central composite design (CCD) for Micro-EDM problems with four EDM variables (peak current, pulse on-time, pulse off-time and electrode rotation speed). Experimental results indicate that peak current is the EDM variable that most affects the Micro-EDM qualities for SK3 carbon tool steel while pulse off-time had a significant interaction with that. The results show that RSM based on the CCD could efficiently be applied for the modeling of Micro-EDM qualities (EW, MRR, and overcut), and it is an economical way to obtain the performance characteristics of Micro-EDM process parameters with the fewest experimental data.

Keywords Response surface method · Central composite design · Electrode wear · Material removal rate · Overcut · Microelectrical discharge machining

Y. C. Lin · S. K. Hung
Department of Mechanical Engineering,
National Chiao Tung University,
Taiwan, Republic of China

C. C. Tsao
Department of Mechatronic Engineering,
Tahua Institute of Technology,
Taiwan, Republic of China

C. Y. Hsu
Department of Mechanical Engineering,
Lunghwa University of Science and Technology,
Taiwan, Republic of China

D. C. Wen (✉)
Department of Mechanical Engineering,
China University of Science and Technology,
Taiwan, Republic of China
e-mail: dcwen@cc.cust.edu.tw

1 Introduction

EDM is a complex process characterized by the use of electric-thermal energy to remove material from the machined areas, regardless of material hardness. Micro-EDM uses EDM for micro manufacturing. Micro-EDM using small energy levels (<100 μJ) has been the focus of intensive research in recent years in order to improve the quality of the finish, because it is an effective machining operation for the production of microholes and microslots in the production of mold inserts for microstructures. The supplied energy in Micro-EDM depends on the discharge voltage, the peak current and the pulse duration in Micro-EDM [1]. However, machining defects, such as electrode wear (EW) and overcut, occur during the Micro-EDM process leading to a lack of machining accuracy in the geometry of workpiece. SK3 carbon tool steel is widely used in the dies and molds, machine parts and cutting tools because of its high toughness and excellent wear resistance. Son et al. [1] reported that a shorter EDM pulse makes a precision part more efficiently with a higher MRR. Han et al. [2] showed that shortening the pulse on-time is more efficient than reducing the peak current in achieving a high quality machined surface. Egashira et al. [3] found that EDM with ultralow discharge energy (voltages <40 V) has the advantage of a low wear ratio, as well as a high machining accuracy. Liu et al. [4]

pointed out that small input energy pulses and high precision systems are the two major requirements on Micro-EDM. Peng et al. [5] combined Micro-EDM deposition with a microreversible EDM selective removal process to fabricate micrometal structures. Pham et al. [6] pointed out that errors from different sources such as the accuracy and repeatability of positioning of the machine, electrode dressing, jigs and fixtures, and electrode wear directly affect the accuracy of the Micro-EDM process. Wong et al. [7] reported that the volume and size of microcraters using single RC-pulse discharges are more consistent for lower-energy than for higher-energy discharges. Aligiri et al. [8] proposed a new tool wear compensation method to solve the problem of geometrical inaccuracy of machined hole depth in Micro-EDM.

Response surface methodology (RSM) is an effective technique for developing, improving, and optimizing processes, which is often used to combine several independent variables and assess how their complex interactions affect desired responses [9, 10]. RSM uses statistical design of experiment techniques, such as the central composite design (CCD) and least-squares fit in the model generation phase. The performance of the proposed model is then demonstrated using checking tests provided by analysis of variance. Response surface plots can be used to investigate the surfaces and locate the optimum condition. A number of researchers have used RSM to evaluate the results and efficiency of manufacturing operations [11–15].

In this study, a method using a relatively small number of experimental trials was used to investigate Micro-EDM process characteristics (EW, MRR, and overcut). Using concepts from design of experiment, a CCD approach is proposed to determine the required number of experimental trials and the locations of the Micro-EDM process characteristics. The experimental trials are performed in the MINITAB (Minitab Inc.) Release 14.0 statistical software. Regression analysis is used to build the statistical models with the variable of interest and the Micro-EDM process characteristics. These models are also used as objective functions for the optimization problems.

2 Experimental design and central composite design

An effective alternative to the factorial design is the CCD, originally developed by Box and Wilson [16], and improved upon by Box and Hunter [17]. The CCD gives almost as much information as a three-level factorial, requires much fewer tests than the full factorial and has been shown to be sufficient to describe the majority of steady-state process responses [18, 19]. For four variables (n=4), the central composite design can be represented by points on a cube, each axis corresponding to a factor represents thirty experiments, consisting of 2^n (2^4=16) factor points, $2n$ (2×4=8) axial points and six center points (six replications). The codes are calculated as functions of the range of interest of each variable based on the preliminary experiments, as shown in Table 1.

When the response data are obtained from the test, a regression analysis is performed to determine the coefficients of the response model and their standard errors and significance. In general, a second-order polynomial response surface mathematical model is used to analyze the parametric influences of the parameters on the various response criteria. The second-order model demonstrates the second-order effect of each variable, separately, and the two-way interaction between combinations of these variables. This second-order mathematical model can be represented as follows:

$$Y = b_o + \sum_{i=1}^{n} b_i X_i + \sum_{i=1}^{n} b_{ii} X_{ii}{}^2 + \sum_{i<j} b_{ij} X_i X_j + \varepsilon \qquad (1)$$

where Y is the corresponding response, X_i is the input variables, X_{ii}^2 and X_iX_j are the squares and interaction terms of these input variables, b_o, b_i, b_{ij}, and b_{ii} are the regression coefficients of the parameters, and ε is the experimental error. All 30 experimental runs for the CCD were performed as shown in Table 2. Table 2 shows that the central composite design composes four independent variables; X (peak current (X_1), pulse on-time (X_2), pulse off-time (X_3) and electrode rotation speed (X_4)), and the response, Y (electrode wear (Y_1), material removal rate (Y_2) and overcut (Y_3)).

3 Experimental procedures

The workpiece material used for the experiments was SK3 carbon tool steel (3 mm in thickness), which was ground with a diamond-grain resin-bond grinding wheel to produce parallel faces. The tool electrode material was tungsten carbide. Tungsten carbide tools were dressed from 0.3 to 0.2 mm diameter using a very accurate CNC grinding machine. A series of experiments on a microgroove of 0.5 mm length and 0.02 mm depth were carried out on an EDM machine (OCT 200-MA, Ocean Technologies) that used an iso-frequent pulse generator, with a maximum operating discharge current of 3A and the capability to set open-circuit voltage at 10 V. The maximum travel of the machine was 200 mm (X)×150 mm (Y)×150 mm (Z) with a positional resolution of 0.1 μm, in the X, Y, and Z directions and a fully closed feedback control to ensure sub-micron accuracy. The overcut was measured using an automatic vision inspector (MTCRO.VU InSpec).

During the Micro-EDM process, the electrode diameter was maintained at a constant value. Therefore, the

Table 1 Parameters and levels for Micro-EDM

Workpiece		SK3 carbon tool steel thickness=3 mm		
Electrode		Tungsten carbide diameter=0.2 mm		
Dielectric fluid		Kerosene		
Polarity		Electrode negative		
		Workpiece positive		
Symbol	Factors	Levels		
		−1	0	+1
X_1	Peak current (mA)	0.3	0.5	1.0
X_2	Pulse on-time (μs)	6	13	25
X_3	Pulse off-time (μs)	3	6	13
X_4	Electrode rotation speed (rpm)	100	300	500

Table 2 Experimental results for EW, MRR and overcut

Std	Actual factors				Response variables					
	X_1	X_2	X_3	X_4	Y_1 (mm)		$Y_2\times10^{-5}$ (mm^3/min)		Y_3 (mm)	
					Observed	Predicted	Observed	Predicted	Observed	Predicted
1	0.3	6	3	100	0.039	0.038	1.721	2.094	0.0098	0.0090
2	1	6	3	100	0.060	0.054	5.319	5.506	0.0174	0.0190
3	0.3	25	3	100	0.039	0.044	1.879	1.792	0.0081	0.0069
4	1	25	3	100	0.083	0.064	4.681	5.366	0.0245	0.0229
5	0.3	6	13	100	0.046	0.039	1.483	1.939	0.0141	0.0138
6	1	6	13	100	0.213	0.197	2.410	2.575	0.0142	0.0147
7	0.3	25	13	100	0.043	0.018	1.659	2.417	0.0121	0.0147
8	1	25	13	100	0.150	0.179	4.104	3.216	0.0217	0.0217
9	0.3	6	3	500	0.039	0.022	3.451	4.254	0.0107	0.0116
10	1	6	3	500	0.045	0.059	9.414	8.348	0.0257	0.0230
11	0.3	25	3	500	0.045	0.055	5.752	5.229	0.0117	0.0103
12	1	25	3	500	0.085	0.095	9.697	9.487	0.0254	0.0278
13	0.3	6	13	500	0.041	0.048	2.815	1.891	0.0080	0.0100
14	1	6	13	500	0.226	0.226	2.782	3.209	0.0104	0.0123
15	0.3	25	13	500	0.042	0.053	3.697	3.646	0.0119	0.0118
16	1	25	13	500	0.254	0.234	5.010	5.128	0.0207	0.0202
17	0.3	13	6	300	0.041	0.055	2.994	2.188	0.0139	0.0123
18	1	13	6	300	0.125	0.126	4.592	5.169	0.0241	0.0225
19	0.5	6	6	300	0.109	0.129	3.339	2.918	0.0130	0.0099
20	0.5	25	6	300	0.146	0.141	3.342	3.535	0.0110	0.0109
21	0.5	13	3	300	0.134	0.133	4.562	4.397	0.0063	0.0091
22	0.5	13	13	300	0.160	0.176	2.697	2.633	0.0152	0.0092
23	0.5	13	6	100	0.104	0.139	3.980	2.327	0.0087	0.0079
24	0.5	13	6	500	0.166	0.146	3.067	4.491	0.0117	0.0093
25	0.5	13	6	300	0.149	0.146	3.263	3.201	0.0085	0.0099
26	0.5	13	6	300	0.171	0.146	2.695	3.201	0.0073	0.0099
27	0.5	13	6	300	0.152	0.146	3.045	3.201	0.0081	0.0099
28	0.5	13	6	300	0.146	0.146	2.953	3.201	0.0090	0.0099
29	0.5	13	6	300	0.163	0.146	3.347	3.201	0.0084	0.0099
30	0.5	13	6	300	0.149	0.146	3.222	3.201	0.0084	0.0099

Table 3 Analysis of variance for EW

Source	Sum of squares	Degree of freedom	Mean square	F value	p value>F	
Model	0.1099	14	0.0078	17.158	< 0.0001	Significant
X_1	0.0443	1	0.0443	96.850	< 0.0001	Significant
X_2	0.0002	1	0.0002	0.497	0.4916	
X_3	0.0221	1	0.0221	48.419	< 0.0001	Significant
X_4	0.0017	1	0.0017	3.847	0.0687	
X_1^2	0.0126	1	0.0126	27.703	< 0.0001	Significant
X_2^2	0.0004	1	0.0004	0.927	0.3507	
X_3^2	7.02E−07	1	7.02E−07	0.001	0.9693	
X_4^2	3.73E−05	1	3.73E−05	0.081	0.7789	
X_1X_2	8.68E−06	1	8.68E−06	0.018	0.8923	
X_1X_3	0.0207	1	0.0207	45.270	< 0.0001	Significant
X_1X_4	0.0004	1	0.0004	0.903	0.3568	
X_2X_3	0.0007	1	0.0007	1.683	0.2141	
X_2X_4	0.0006	1	0.0006	1.476	0.2431	
X_3X_4	0.0005	1	0.0005	1.283	0.2750	
Residual	0.0068	15	0.0004			
Lack of fit	0.0063	10	0.0006	6.62	0.0250	
Pure error	0.0004	5	0.00009			
Correlation total	0.1168	29				

EW and MRR for the Micro-EDM operation were calculated using Eqs. 2 and 3, respectively, which are shown below:

$$\mathrm{EW} = A_S \Delta L \tag{2}$$

$$\mathrm{MRR} = A_S F_O \tag{3}$$

where ΔL is the distance between an ideal blind hole and machined blind hole in micrometers, A_S is the area of electrode in square micrometers and F_O is the cutting feed in micrometers per minute for Micro-EDM.

Table 4 Analysis of variance for MRR

Source	Sum of squares	Degree of freedom	Mean square	F value	p value>F	
Model	9.24E−09	14	6.60E−10	8.42	< 0.0001	Significant
X_1	2.69E−09	1	2.69E−09	34.25	< 0.0001	Significant
X_2	2.93E−10	1	2.93E−10	3.73	0.0724	
X_3	2.28E−09	1	2.28E−09	29.13	< 0.0001	Significant
X_4	1.86E−09	1	1.86E−09	23.66	0.0002	Significant
X_1^2	6.56E−12	1	6.56E−12	0.084	0.7764	
X_2^2	8.13E−13	1	8.13E−13	0.010	0.9203	
X_3^2	1.12E−10	1	1.12E−10	1.43	0.2499	
X_4^2	1.12E−11	1	1.12E−11	0.14	0.7110	
X_1X_2	2.73E−12	1	2.73E−12	0.035	0.8544	
X_1X_3	8.00E−10	1	8.00E−10	10.20	0.0060	Significant
X_1X_4	4.76E−11	1	4.76E−11	0.61	0.4483	
X_2X_3	6.25E−11	1	6.25E−11	0.80	0.3862	
X_2X_4	1.65E−10	1	1.65E−10	2.10	0.1681	
X_3X_4	4.96E−10	1	5.00E−10	6.33	0.0238	
Residual	1.18E−09	15	7.84E−11			
Lack of fit	1.15E−09	10	1.15E−10	19.77	0.0021	
Pure error	2.90E−11	5	5.80E−12			
Correlation total	1.04E−08	29				

Table 5 Analysis of variance for overcut

Source	Sum of squares	Degree of freedom	Mean square	*F* value	*p* value>*F*	
Model	0.00088	14	6.34E−05	7.89	0.0001	Significant
X_1	3.79E−04	1	3.79E−04	47.22	< 0.0001	Significant
X_2	3.65E−05	1	3.65E−05	4.54	0.0499	
X_3	9.12E−06	1	9.12E−06	1.13	0.3036	
X_4	1.24E−06	1	1.24E−06	0.15	0.6999	
X_1^2	7.02E−05	1	7.02E−05	8.74	0.0098	Significant
X_2^2	3.06E−07	1	3.06E−07	0.03	0.8479	
X_3^2	1.62E−06	1	1.62E−06	0.20	0.6597	
X_4^2	4.57E−06	1	4.57E−06	0.56	0.4623	
X_1X_2	3.79E−05	1	3.79E−05	4.71	0.0463	
X_1X_3	8.46E−05	1	8.46E−05	10.53	0.0054	Significant
X_1X_4	1.93E−06	1	1.93E−06	0.24	0.6309	
X_2X_3	9.41E−06	1	9.41E−06	1.17	0.2962	
X_2X_4	8.04E−07	1	8.04E−07	0.10	0.7560	
X_3X_4	4.11E−05	1	4.11E−05	5.12	0.0389	
Residual	1.20E−04	15	8.03E−06			
Lack of fit	0.00011	10	1.18E−05	37.46	0.0004	
Pure error	1.58E−06	5	3.17E−07			
Correlation total	0.00100	29				

4 Results and discussion

4.1 Analysis of variance and fitted regression models

A series of experiments was performed using a CCD, as shown in Table 2. Various statistical data (standard error of estimate, sum of squares of the errors, *F* statistics, and *p* value) for EW, MRR, and overcut in Micro-EDM were examined. Using 5% and 1% significance levels, a model was considered significant if the *p* value (significance probability value) was less than 0.05 and 0.001, respectively. From these *p* values for EW, presented in Table 3, it can be seen that the effects of X_1, X_3, X_1^2 and X_1X_3 were statistically significant. From the *p* values for MRR, shown

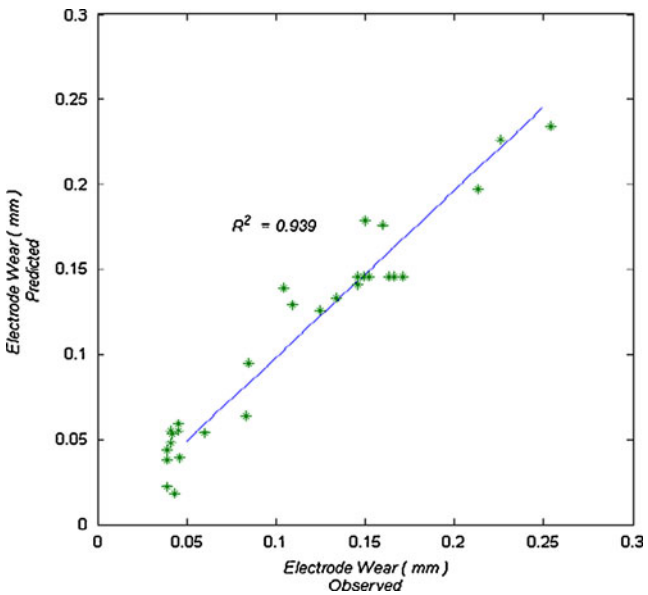

Fig. 1 Relationship between experimental and predicted electrode wear for Micro-EDM using Eq. 4

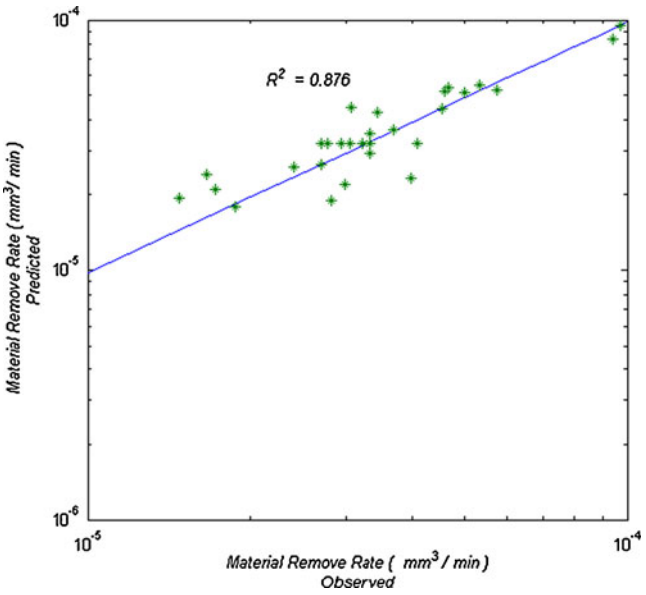

Fig. 2 Relationship between experimental and predicted material removal rate for Micro-EDM using Eq. 5

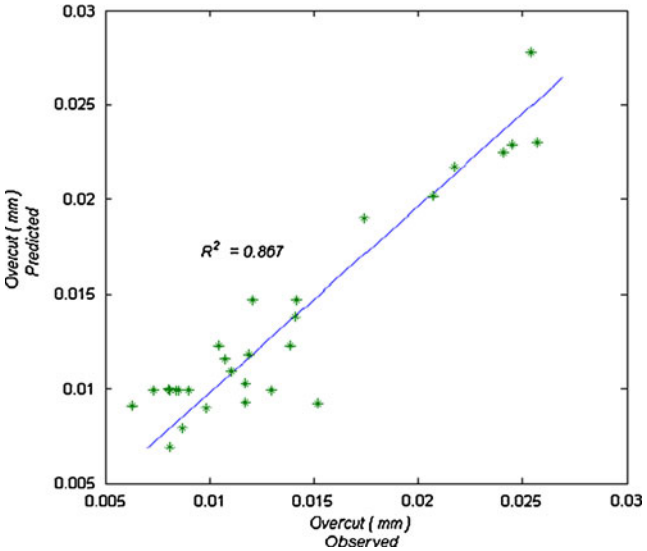

Fig. 3 Relationship between experimental and predicted overcut for Micro-EDM using Eq. 6

in Table 4, it can be seen that the effects of X_1, X_3, and X_4 were statistically significant. From the p values for overcut, reported in Table 5, it can be seen that the effect of X_1 was statistically significant. However, of these four variables, peak current (X_1) was the major factor affecting the Micro-EDM qualities of SK3 carbon tool steel while pulse off-time (X_3) had a significant interaction.

From the experimental design and the results in Table 2, the second-order response functions representing electrode wear (Y_1), material removal rate (Y_2) and overcut (Y_3) of SK3 carbon tool steel can be expressed as a function of four operating parameters for the Micro-EDM, namely peak current (X_1), pulse on-time (X_2), pulse off-time (X_3), and electrode rotation speed (X_4). The relationship between the responses (EW, MRR, and overcut of SK3 carbon tool steel) and operating parameters were obtained for a coded unit as follows:

EW model equation:

$$\begin{aligned} Y_1 = {} & -0.188 + 0.878X_1 + 5.117\times10^{-3}X_2 - 5.252\times10^{-3}X_3 - 4.104\times10^{-5}X_4 \\ & -0.710{X_1}^2 - 1.533\times10^{-4}{X_2}^2 - 2.510\times10^{-5}{X_3}^2 - 9.501\times10^{-8}{X_4}^2 \\ & +2.185\times10^{-4}X_1X_2 + 2.018\times10^{-2}X_1X_3 + 7.193\times10^{-5}X_1X_4 \\ & -1.443\times10^{-4}\,X_2X_3 + 3.408\times10^{-6}X_2X_4 + 6.008\times10^{-6}X_3X_4 \quad (\text{mm}) \end{aligned} \tag{4}$$

MRR model equation:

$$\begin{aligned} Y_2 = {} & 8.946\times10^{-6} + 7.844\times10^{-5}X_1 - 2.793\times10^{-7}X_2 - 3.74\times10^{-6}X_3 + 2.2\times10^{-8}X_4 \\ & -1.614\times10^{-5}{X_1}^2 - 6.707\times10^{-9}{X_2}^2 + 3.175\times10^{-7}{X_3}^2 + 5.194\times10^{-11}{X_4}^2 \\ & +1.226\times10^{-7}X_1\,X_2 - 3.965\times10^{-6}X_1X_3 + 2.438\times10^{-8}X_1X_4 \\ & +4.108\times10^{-8}X_2X_3 + 1.681\times10^{-9}X_2X_4 - 5.521\times10^{-9}X_3X_4 \quad (\text{mm}^3/\text{min}) \end{aligned} \tag{5}$$

Overcut model equation:

$$\begin{aligned} Y_3 = {} & 1.636\times10^{-2} - 5.378\times10^{-2}X_1 - 4.371\times10^{-4}X_2 + 1.536\times10^{-3}X_3 + 2.896\times10^{-5}X_4 \\ & +5.284\times10^{-2}{X_1}^2 + 4.117\times10^{-6}{X_2}^2 - 3.816\times10^{-5}{X_3}^2 - 3.323\times10^{-8}{X_4}^2 \\ & +4.568\times10^{-4}X_1X_2 - 1.29\times10^{-3}X_1X_3 + 4.918\times10^{-6}X_1X_4 \\ & +1.595\times10^{-5}X_2X_3 + 1.176\times10^{-7}X_2X_4 - 1.59\times10^{-6}X_3X_4 \quad (\text{mm}) \end{aligned} \tag{6}$$

The response factors for any regime within the interval of the selected experimental design can be calculated from Eqs. 4 to 6. The predicted values obtained using model equations (Eqs. 4, 5, and 6) are shown in Figs. 1, 2, and 3, respectively. It is clear that the predicted values match the experimental values reasonably well with R^2 of 0.939 for EW, R^2 of 0.876 for MRR, and R^2 of 0.867 for overcut of SK3 carbon tool steel for Micro-EDM.

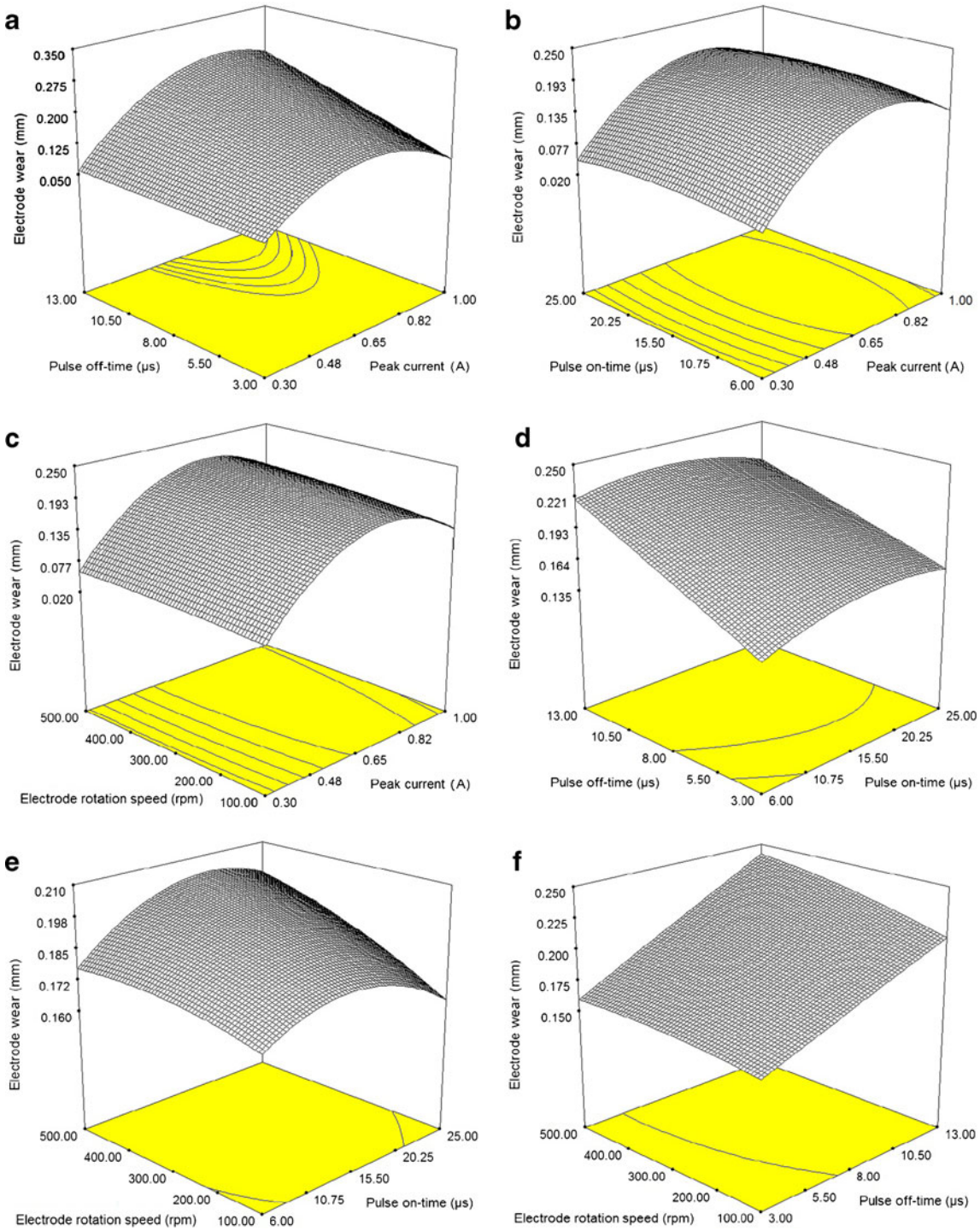

Fig. 4 Response surface plots showing the effect of two variables on the EW of Micro-EDM. The other two variables are maintained at the middle level. **a** Pulse off-time and peak current; **b** pulse on-time and peak current; **c** electrode rotation speed and peak current; **d** pulse off-time and pulse on-time; **e** electrode rotation speed and pulse on-time and **f** electrode rotation speed and pulse off-time

4.2 Effect of the Micro-EDM variables on EW

The response surface plots, shown in Fig. 4, demonstrate the effect of different Micro-EDM variables on EW. The figures show the relationship between two Micro-EDM variables and electrode wear at the middle level of the other two variables. Figure 4a shows the effect of pulse off-time and peak current on EW. A lower pulse off-time and a lower peak current have a minor effect on EW, but it is worth noting that larger EW occurs for the center level of

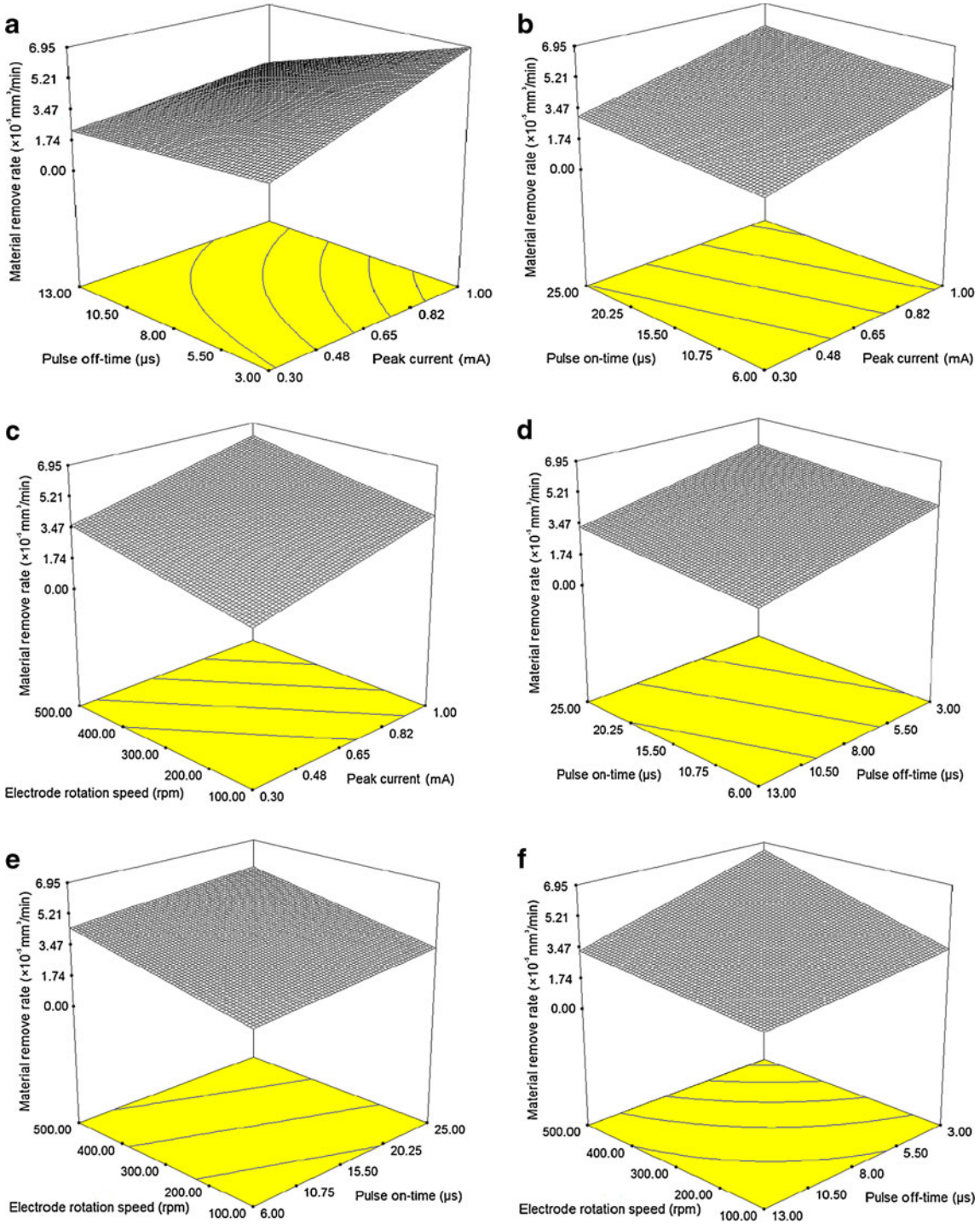

Fig. 5 Response surface plots showing the effect of two variables on the MRR of Micro-EDM. The other two variables are maintained at the middle level. **a** Pulse off-time and peak current; **b** pulse on-time and peak current; **c** electrode rotation speed and peak current; **d** pulse off-time and pulse on-time; **e** electrode rotation speed and pulse on-time and **f** electrode rotation speed and pulse off-time

the peak current. Figure 4b shows the effect of pulse on-time and peak current on EW. It can be seen that EW depends more on the peak current than on pulse on-time. It is also worth noting that lower EW occurs for a lower peak current. Figure 4c shows the effect of electrode rotation speed and peak current on EW. The general form of the three-dimensional (3D) relationship is similar to that of the previous figure. Figure 4d shows the effect of pulse off-time and pulse on-time on EW. A minor EW occurs for minimum level pulse off-time and pulse on-time. Figure 4e

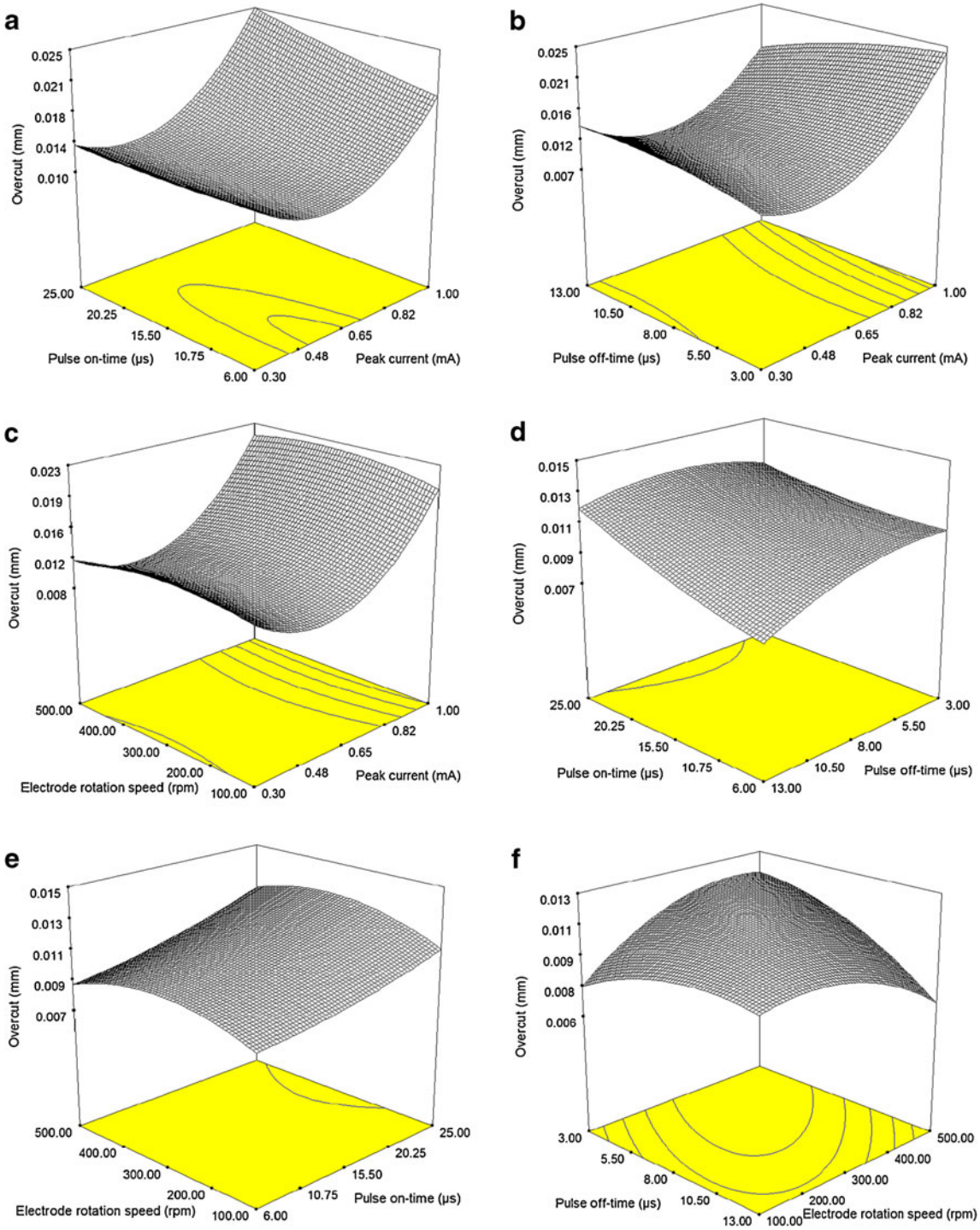

Fig. 6 Response surface plots showing the effect of two variables on the overcut of Micro-EDM. The other two variables are maintained at the middle level. **a** Pulse off-time and peak current; **b** pulse on-time and peak current; **c** electrode rotation speed and peak current; **d** pulse off-time and pulse on-time; **e** electrode rotation speed and pulse on-time and **f** electrode rotation speed and pulse off-time

shows the effect of electrode rotation speed and pulse on-time on EW. The general form of the 3D relationships is similar to that shown in Fig. 4a–c. EW depends more on the pulse on-time than on electrode rotation speed. It is clear that lower EW occurs for a lower pulse on-time and lower electrode rotation speed. Figure 4f shows the effect of electrode rotation speed and pulse off-time on EW. A minor EW occurs for the minimum level of electrode rotation speed and pulse off-time. It can be seen that EW depends more on the pulse off-time than on electrode rotation speed.

4.3 Effect of Micro-EDM variables on MRR

Figure 5 shows the response surface plots for two Micro-EDM variables and MRR at the middle level for the other two variables. Figure 5a shows the effect of pulse off-time and peak current on MRR. It can be seen that maximum MRR occurs for a minimum level pulse off-time, but a maximum peak current level. Peak current has a significant effect on MRR whilst pulse off-time has a trivial effect. Figure 5b reports the effect of pulse on-time and peak current on MRR. It can be seen that maximum MRR occurs for a maximum level pulse on-time and maximum peak current level, but the effect of the peak current is more powerful than that of the pulse on-time. Figure 5c shows the effect of electrode rotation speed and peak current on MRR. The general form of the 3D relationship is similar to that of the previous figure. Figure 5d shows the effect of pulse off-time and pulse on-time on MRR. Both variables have the same effect on MRR. As the pulse off-time or on-time is increased, MRR is increased. Figure 5e shows the effect of electrode rotation speed and pulse on-time on MRR. It is clear that, as the electrode rotation speed increases, MRR increases steadily. It can be seen that MRR depends more on the electrode rotation speed rather than on pulse on-time. Figure 5f shows the effect of electrode rotation speed and pulse off-time on MRR. It is of note that the general form of the 3D relationship is similar to that of the previous figure. Namely, as the electrode rotation speed is increased, MRR is increased and when the pulse off-time is increased, MRR is increased progressively.

4.4 Effect of Micro-EDM variables on overcut

The response surface plots, as shown in Fig. 6, demonstrate the effect of different Micro-EDM variables on overcut. Figure 6a shows the effect of pulse off-time and peak current on overcut. Minimum overcut occurs for a minimum level pulse off-time and a middle level of peak current. It is clear from Fig. 6a that the middle level of peak current is best for lower overcut. Figure 6b shows the effect of pulse on-time and peak current on overcut. It can be seen that minimum overcut occurs for a minimum level pulse on-time and middle level of peak current, but the effect of peak current is greater than that of pulse on-time. Figure 6c shows the effect of electrode rotation speed and peak current on overcut. The general form of the 3D relationship is similar to that of the previous figure. Figure 6d shows the effect of pulse off-time and pulse on-time on overcut. Both variables have a non-liner effect on overcut. As the pulse off-time is increased, overcut is increased, as it is for an increase in pulse on-time. Figure 6e presents the effect of electrode rotation speed and pulse on-time on overcut. An increased pulse on-time does not cause a lower overcut at the center level of electrode rotation speed. Figure 6f shows the effect of electrode rotation speed and pulse off-time on overcut. It is clear that as the pulse off-time is decreased, overcut is decreased progressively, and that the middle level of electrode rotation speed is not a good condition for lower overcut but the extreme levels are good.

5 Summary and conclusion

The use of RSM and CCD for modeling the influence of four machining variables (namely, peak current, pulse on-time, pulse off-time, and electrode rotation speed) on the performance of the Micro-EDM machined SK3 carbon tool steel was evaluated. The predicted values match the experimental values reasonably well with R^2 of 0.939 for EW, R^2 of 0.876 for MRR, and R^2 of 0.867 for overcut. This study demonstrates that CCD and RSM can be successfully used to model some machining parameters of the Micro-EDM process for SK3 carbon tool steel using the fewest possible number of experiments. Findings from this study, however, indicate that peak current (X_1) is the significant factor of the four machining variables that affects Micro-EDM qualities for SK3 carbon tool steel. Lower peak current minimizes the EW and overcut, and maximizes the MRR, but decreased pulse on-time and increased electrode rotation speed, considerably, which is necessary to induce more discharge energy for lower EW, higher MRR and lower overcut.

References

1. Son SM, Lim HS, Kumar AS, Rahman M (2007) Influences of pulsed power condition on the machining properties in micro EDM. J Mater Process Technol 190:73–76
2. Han F, Jiang J, Yu D (2007) Influence of machining parameters on surface roughness in finish cut of WEDM. Int J Adv Manuf Technol 34:538–546
3. Egashira K, Matsugasako A, Tsuchiya H, Miyazaki M (2006) Electrical discharge machining with ultralow discharge energy. Precis Eng 30(4):414–420
4. Liu K, Lauwers B, Reynaerts D (2010) Process capabilities of Micro-EDM and its applications. Int J Adv Manuf Technol 47:11–19
5. Peng ZL, Wang ZL, Dong YH, Chen H (2010) Development of a reversible machining method for fabrication of microstructures by using micro-EDM. J Mater Process Technol 210:129–136
6. Pham DT, Dimov SS, Bigot S, Ivanov A, Popov K (2004) Micro-EDM—recent developments and research issues. J Mater Process Technol 149:50–57
7. Wong YS, Rahman M, Lim HS, Han H, Ravi N (2003) Investigation of micro-EDM material removal characteristics using single RC-pulse discharges. J Mater Process Technol 140:303–307
8. Aligiri E, Yeo SH, Tan PC (2010) A new tool wear compensation method based on real-time estimation of material removal volume in micro-EDM. J Mater Process Technol 210:2292–2303

9. Kilickap E, Huseyinoglu M, Yardimeden A (2011) Optimization of drilling parameters on surface roughness in drilling of AISI 1045 using response surface methodology and genetic algorithm. Int J Adv Manuf Technol 52:79–88
10. Natarajan U, Periyanan PR, Yang SH (2011) Multiple-response optimization for micro-endmilling process using response surface methodology. Int J Adv Manuf Technol 56:177–185
11. Djoudi W, Aissani-Benissad F, Bourouina-Bacha S (2007) Optimization of copper cementation process by iron using central composite design experiments. Chem Eng J 133:1–6
12. Aslan N (2008) Application of response surface methodology and central composite rotatable design for modeling and optimization of a multi-gravity separator for chromite concentration. Powder Technol 185:80–86
13. Sohani MS, Gaitonde VN, Siddeswarappa B, Deshpande AS (2009) Investigations into the effect of tool shapes with size factor consideration in sink electrical discharge machining (EDM) process. Int J Adv Manuf Technol 45:1131–1145
14. Tsao CC (2008) Comparison between response surface methodology and radial basis function network for core-center drill in drilling composite materials. Int J Adv Manuf Technol 37:1061–1068
15. Hang Y, Qu M, Ukkusuri S (2011) Optimizing the design of a solar cooling system using central composite design techniques. Energy Build 43:988–994
16. Box GEP, Wilson KB (1951) On the experimental attainment of optimum conditions. J R Stat Soc Ser B-Stat Methodol 13:1–45
17. Box GEP, Hunter JS (1957) Multi-factor experimental design for exploring response surfaces. Ann Math Stat 28:195–241
18. Obeng DP, Morrell S, Napier TJN (2005) Application of central composite rotatable design to modeling the effect of some operating variables on the performance of the three-product cyclone. Int J Miner Process 769:181–192
19. Crozier RD (1992) Flotation theory, reagents and ore testing. Pergamon, New York